

# Estrogen increases synaptic connectivity between single presynaptic inputs and multiple postsynaptic CA1 pyramidal cells: A serial electron-microscopic study

Maya Yankova, Sharron A. Hart, and Catherine S. Woolley\*

Department of Neurobiology and Physiology, Northwestern University, Evanston, IL 60208

Communicated by Bruce S. McEwen, The Rockefeller University, New York, NY, December 28, 2000 (received for review December 12, 2000)

Dendritic spines are sites of the vast majority of excitatory synaptic input to hippocampal CA1 pyramidal cells. Estrogen has been shown to increase the density of dendritic spines on CA1 pyramidal cell dendrites in adult female rats. In parallel with increased spine density, estrogen has been shown also to increase the number of spine synapses formed with multiple synapse boutons (MSBs). These findings suggest that estrogen-induced dendritic spines form synaptic contacts with preexisting presynaptic boutons, transforming some previously single synapse boutons (SSBs) into MSBs. The goal of the current study was to determine whether estrogen-induced MSBs form multiple synapses with the same or different postsynaptic cells. To quantify same-cell vs. different-cell MSBs, we filled individual CA1 pyramidal cells with biocytin and serially reconstructed dendrites and dendritic spines of the labeled cells, as well as presynaptic boutons in synaptic contact with labeled and unlabeled (i.e., different-cell) spines. We found that the overwhelming majority of MSBs in estrogen-treated animals form synapses with more than one postsynaptic cell. Thus, in addition to increasing the density of excitatory synaptic input to individual CA1 pyramidal cells, estrogen also increases the divergence of input from individual presynaptic boutons to multiple postsynaptic CA1 pyramidal cells. These findings suggest the formation of new synaptic connections between previously unconnected hippocampal neurons.

Previous studies have shown that estrogen increases the density of synaptic input to hippocampal CA1 pyramidal cells in adult female rats. The density of both dendritic spines (e.g., refs. 1 and 2) and spine synapses (3) on CA1 pyramidal cells is greater in ovariectomized estrogen-treated rats than in ovariectomized controls. Consistent with the fact that dendritic spines are sites of excitatory input, electrophysiological studies show that the estrogen-induced increase in spine density is paralleled by enhanced sensitivity of CA1 pyramidal cells to excitatory synaptic input (4).

Based on a serial electron-microscopic study of presynaptic boutons and postsynaptic dendritic spines, Woolley *et al.* (5) proposed that new spines induced by estrogen form synapses primarily with preexisting presynaptic boutons. This suggestion was based on the following argument. Presynaptic boutons afferent to CA1 dendritic spines can be divided into 2 classes (6): single synapse boutons (SSBs), which are synaptically connected to one dendritic spine and multiple synapse boutons (MSBs), which are synaptically connected to more than one spine. Analysis of CA1 presynaptic boutons showed an estrogen-induced increase in the relative frequency of MSBs to SSBs as well as an increase in the average number of synapses each MSB forms (5). Using these data, Woolley and colleagues calculated that for any given number of presynaptic boutons, there were 25% more synapses formed on CA1 spines in estrogen-treated animals. This value is very similar to the percentage increase in dendritic spine/synapse density induced by estrogen, indicating

that additional presynaptic boutons are not needed to accommodate estrogen-induced dendritic spines. These observations suggested that estrogen-induced spines form synapses with preexisting boutons, transforming some previously SSBs into MSBs, as well as adding synapses to existing MSBs.

However, Woolley *et al.* (5) could not determine whether estrogen-induced spines form synapses with presynaptic boutons that are already synaptically connected to the same postsynaptic cell as the new spine or alternatively, whether new spines form synapses with presynaptic boutons that are synaptically connected to a different postsynaptic cell(s). The answer to this question has important implications for the functional consequences of new spine/synapse formation. The first possibility, increased numbers of "same-cell" contacts, predicts increased efficiency of synaptic transmission between a presynaptic input and a postsynaptic cell. In this case, action potential invasion of a single presynaptic bouton would be more likely to depolarize a postsynaptic cell, because it would have more than one synaptic contact with that cell. The second possibility, increased numbers of "different-cell" synaptic contacts, predicts increased synchronization of synaptically driven activity in CA1. In this second case, action potential invasion of a single presynaptic bouton would have the possibility of coincident depolarization of more than one postsynaptic cell.

To determine whether MSB synaptic contacts on CA1 pyramidal cells are same-cell or different-cell, we studied the synaptic connections of identified dendrites from estrogen-treated and control animals. Individual CA1 pyramidal cells were filled with biocytin so that all the dendrites and spines on that one cell would be identifiable in electron micrographs. We then serially reconstructed dendritic segments of filled cells, their filled spines, all presynaptic boutons in contact with those filled spines, and any additional unfilled dendritic spines (i.e., those from a different cell) in synaptic contact with those boutons.

Here we report that the overwhelming majority of CA1 MSBs in estrogen-treated animals forms synapses with more than one postsynaptic cell. This change increases the number of sites at which different postsynaptic cells share input from single presynaptic boutons and may reflect the establishment of new synaptic connections between previously unconnected cells.

## Materials and Methods

**Animal Treatment.** Adult female Sprague–Dawley rats (250–275 g) were housed on a 12-h light/dark cycle with unlimited access to food and water. These animals were ovariectomized (OVX) and

Abbreviations: SSB, single synapse bouton; MSB, multiple synapse bouton; OVX, ovariectomized.

See commentary on page 2956.

\*To whom reprint requests should be addressed. E-mail: cwoolley@northwestern.edu.

The publication costs of this article were defrayed in part by page charge payment. This article must therefore be hereby marked "advertisement" in accordance with 18 U.S.C. §1734 solely to indicate this fact.

treated with estradiol benzoate by using the same treatment protocol previously shown to regulate dendritic spine and axospinous synapse density on hippocampal CA1 pyramidal cells (1–3). Briefly, rats were ovariectomized under Metofane anesthesia. On the 3rd and 4th days after surgery, each received s.c. injections of either 10  $\mu$ g 17 $\beta$ -estradiol benzoate in 100  $\mu$ l sesame oil (OVX + E) or 100  $\mu$ l of oil vehicle alone (OVX + O) 24 h apart. Then 48 h after the second estradiol or oil injection, animals were killed by decapitation and hippocampal slices were prepared from their brains.

**Preparation of Hippocampal Slices.** After decapitation, brains were removed quickly, cooled in ice-cold oxygenated (95% O<sub>2</sub>/5% CO<sub>2</sub>) sucrose artificial cerebrospinal fluid (sACSF; in mM 220 sucrose/3 KCl/1.25 NaH<sub>2</sub>PO<sub>4</sub>/2 MgSO<sub>4</sub>/36 NaCO<sub>3</sub>/2 CaCl<sub>2</sub>/10 dextrose) and blocked to contain the dorsal hippocampus. Using a Vibroslicer (Frederick Haer, Brunswick, ME), 400- $\mu$ m thick slices transverse to the long axis of the hippocampus were cut into a bath of oxygenated sACSF at 4°C. Slices then were transferred to a holding chamber, in which they remained in oxygenated ACSF (124 mM NaCl in place of sucrose) at room temperature until used for recording.

Between 30 min and 2 h after cutting, slices were transferred individually to an interface recording chamber, in which they rested on a nylon mesh over a well that was perfused ( $\approx$ 1 ml/min) with oxygenated artificial cerebrospinal fluid at 34.5°C. Warmed humidified air was circulated above the slices. Slices remained undisturbed in the chamber for an additional 30 min before recording.

**Intracellular Recording and Cell Filling.** Recording electrodes made from borosilicate glass were filled with 2% (wt/vol) biocytin dissolved in 1 M potassium acetate (100–200 M $\Omega$ ). Intracellular potentials were recorded by using an Axoclamp 2A amplifier (Axon Instruments, Foster City, CA). Bridge balance was monitored continuously on an oscilloscope. Neurons within the CA1 pyramidal cell layer were impaled and identified tentatively as pyramidal cells based on their response to direct current injection (7); the identity of these cells was confirmed after visualization of injected biocytin. Biocytin was injected iontophoretically by using 300-msec, 0.5- to 1.0-nA hyperpolarizing current pulses delivered every 600 msec for 5–20 min. Slices remained in the recording chamber for 30 min after biocytin injection.

**Tissue Processing.** Slices were removed from the recording chamber and fixed for 4–5 h lying flat between two pieces of filter paper in 2.5% paraformaldehyde/1.25% glutaraldehyde in 0.1 M phosphate buffer at 4°C. After fixation, slices were cryoprotected, sectioned at 60  $\mu$ m on a freezing microtome, and processed for visualization of biocytin. Sections were treated first with 0.5–1.0% H<sub>2</sub>O<sub>2</sub> in Tris buffer (TB) to suppress endogenous peroxidase activity followed by a solution of 2% BSA and 0.25% dimethyl sulfoxide in 0.05 M Tris buffered saline to block nonspecific staining and permeabilize membranes. Next, sections were incubated in an avidin/biotin/horseradish peroxidase solution (Vector Elite ABC kit, 1:500; Vector Laboratories, Burlingame, CA) for 36 h at 4°C. Sections then were preincubated in TB containing 0.025% diaminobenzidine and 0.005% NiNH<sub>4</sub>SO<sub>4</sub> for 20 min in the dark. Finally, 0.002% H<sub>2</sub>O<sub>2</sub> was mixed into the preincubation solution, and the tissue was reacted for 60–120 min in the dark. After the reaction, sections were examined under a microscope to determine whether they contained dendrites of biocytin-labeled CA1 pyramidal cells. Sections with labeled pyramidal cell dendrites were processed further for electron microscopy.

Sections with labeled dendrites were stained for 1 h with 1% osmium tetroxide, dehydrated in graded ethanols, infiltrated with epoxy resin, and flat embedded. An example of an embed-

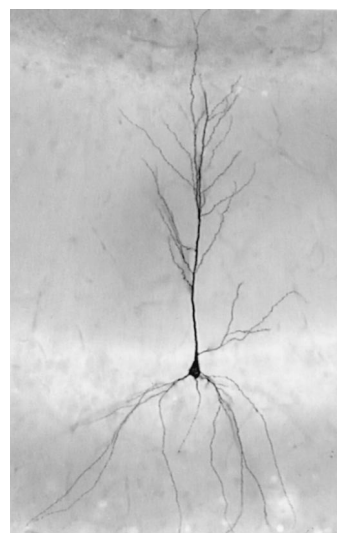


**Fig. 1.** Representative biocytin-filled CA1 pyramidal cell. This image was taken before serial sectioning for electron microscopic analysis.

ded biocytin-filled CA1 pyramidal cell used in this study is shown in Fig. 1. Before further sectioning, a detailed drawing of each cell and nearby tissue landmarks (e.g., blood vessels) was made by using a camera-lucida drawing tube.

Once drawings were made, the CA1 region was dissected from the rest of the section, mounted on a blank epoxy resin capsule, and trimmed to contain the pyramidal cell layer, stratum radiatum, and stratum lacunosum-moleculare. Semithin sections (1- $\mu$ m) were cut and stained with toluidine blue until the first pieces of biocytin-filled dendrite appeared in the sections. Ultrathin sections (light-yellow interference color) then were cut and mounted individually but in order on formvar-coated slot grids. After ultrathin sectioning, grids were stained with 2.5–3% uranyl acetate for 30 min followed by 2.66% Reynold's lead citrate for 5 min and examined on a JEOL 100CX-II electron microscope.

**Electron Microscopy and Three-Dimensional Reconstruction of Dendrites.** Every 5th grid within a series of 200–300 grids was screened initially at  $\times$ 1,900–5,800 until grids containing a suitable segment of biocytin-labeled stratum radiatum dendrite were located. We used the first segment of labeled dendrite that appeared in the series and was: (i) located 150–300  $\mu$ m from the cell body layer; (ii) not part of the 1° dendrite; (iii) relatively thin (0.5- to 1.0- $\mu$ m in diameter); and (iv) roughly parallel to the surface of the tissue block so that it was sectioned longitudinally. Once a potential dendritic segment was identified, pictures were taken ( $\times$ 5,800–10,000) through 45–65 serial sections and printed at  $\times$ 25,800. The distance of each dendritic segment from the cell body layer was measured at  $\times$ 200. The orientation, distance from the cell body layer, and nearby tissue landmarks were used to identify each reconstructed dendrite in its camera-lucida drawing.

For each section in a series, profiles of the biocytin-filled dendritic shaft and spines, presynaptic boutons in contact with filled spines (see below), and any unfilled dendritic spines in synaptic contact with those presynaptic boutons were traced onto individual acetate sheets. Biocytin-labeled structures were identified easily by the presence of electron-dense diaminobenzidine-reaction product. Axospinous presynaptic boutons were membrane-bound profiles containing round clear vesicles. Boutons were judged to be in synaptic contact with the filled cell if two criteria were met: (i) an unambiguous synaptic cleft was visible between the spine and bouton, and (ii) the bouton

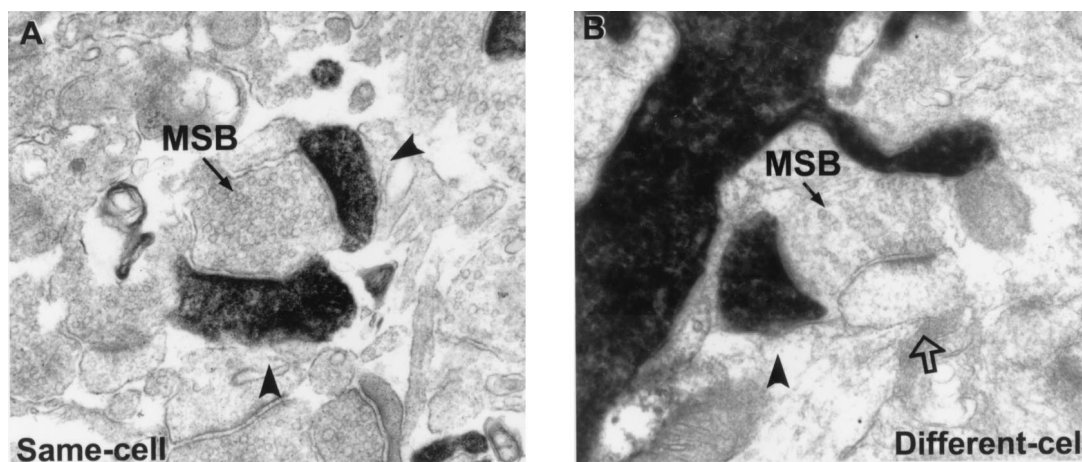


**Fig. 2.** Examples of MSBs that form synapses with multiple filled dendritic spines (A, same-cell) or with a filled spine and an unfilled spine (B, different-cell). Filled arrowheads indicate synaptic contacts with filled spines, and the open arrow indicates a synaptic contact with an unfilled spine.

contained either a presynaptic density adjacent to the synaptic cleft or clustering of at least two round clear vesicles in close proximity to the synaptic cleft. In some but not all cases, a postsynaptic density was visible in the filled spine head. In cases where a spine extended from the dendrite orthogonal to the plane of section, a bouton was judged to be in synaptic contact with the spine if it appeared directly above or below the last section containing the spine head, and no other bouton in synaptic contact with that spine could be identified. Unfilled dendritic spines in synaptic contact with boutons that were also in synaptic contact with the filled cell were identified by the same criteria as filled spine contacts except that a postsynaptic density was virtually always visible in a synaptically connected unfilled spine head. During tracing of these structures, adjacent sections in a series were aligned by using tissue landmarks that were not part of the analysis (e.g., mitochondria and myelinated axons). Nine dendritic segments from four OVX + O and five OVX + E cells were reconstructed. Of the nine series, two contained no missing sections, five were missing one section, and two were missing two (nonadjacent) sections. Any presynaptic boutons that extended beyond the limits of a series were excluded from analysis, because not all their potential postsynaptic partners could be confirmed.

Section thickness was determined by using the method of Harris and Stevens (8). In at least three levels per series, the diameter of a longitudinally sectioned mitochondrion was measured in the section in which it was greatest, the number of sections through which the mitochondrion was sectioned was counted, and the diameter divided by the number of sections. Average section thickness was 82 nm. For computer three-dimensional reconstruction, acetate sheets containing drawings for each section of a series were scanned, aligned, and retraced by using SEM ALIGN and IGL TRACE (courtesy of Kristen Harris and John Fiala, free download from [www.synapses.bu.edu](http://www.synapses.bu.edu)) and imported into 3D STUDIO MAX (AutoDesk, San Raphael, CA).

All quantitative data for a particular dendritic segment were obtained from the aligned tracings through that segment. From these tracings, we determined the (i) true length of the segment, (ii) linear density of dendritic spines, (iii) linear densities, proportions, and locations of SSBs and MSBs; and (iv) numbers of synaptic contacts each MSB formed with filled or unfilled dendritic spines (i.e., multiple same-cell contacts or different-cell contacts). Examples of same-cell and different-cell MSBs that make multiple synaptic contacts in the same section are shown in Fig. 2. It is important to note that all dendrites and spines from one cell were labeled with biocytin, eliminating the

possibility that we would falsely identify a spine as belonging to another cell simply because it originated from a different dendrite.

For statistical comparison of quantitative measurements from OVX + O and OVX + E dendrites, means were calculated for each dendrite and subjected to unpaired two-tailed Student's *t* tests. For analysis of the order of SSB vs. MSB occurrence along the length of each dendrite, we used the Wilcoxon–Mann–Whitney rank sum test for randomness of classes in a sequence. For samples with over 30 observations, the calculated test statistic follows a normal distribution.

## Results

**Dendritic Segments.** Quantitative data for each reconstructed dendritic segment as well as treatment group averages are reported in Table 1. Two segments, one from OVX + O and one from OVX + E, belonged to 2° dendrites, and the remaining segments were part of 3° dendrites. The average length of reconstructed segments was 22.3  $\mu\text{m}$ ; the total length of dendrite reconstructed was 200.7  $\mu\text{m}$ .

Most biocytin-labeled dendritic protrusions had spine-like morphology in that they ended in an enlargement (i.e., a spine head) that contacted a presynaptic bouton. Only approximately 7% of labeled protrusions with apparent spine heads could not be connected to a presynaptic bouton. In addition to dendritic spines, a low density of filopodia-like dendritic protrusions with a tapered ending and no apparent synaptic contact also was observed.

We reconstructed a total of 765 dendritic spines from serial sections of the nine biocytin-filled dendritic segments. Comparison of the density of dendritic spines on dendrites from OVX + O vs. OVX + E animals confirmed previous reports of greater CA1 pyramidal cell spine density in estrogen-treated animals (e.g., refs. 1–3). Considering both 2° and 3° dendrites, the mean density of dendritic spines was 27.6% greater on the OVX + E dendrites than on the OVX + O dendrites, although this difference only represents a statistical trend ( $t = -2.232$ ,  $P = 0.06$ ). However, considering the seven 3° dendrites (3° dendrites have been analyzed in light-microscopic studies, e.g., ref. 1), OVX + E spine density was significantly greater by 29% ( $t = -3.598$ ,  $P = 0.016$ ). In contrast to spine density, the linear density of filopodia-like structures was unchanged by estrogen.

**Presynaptic Boutons.** We also serially reconstructed 709 presynaptic boutons in synaptic contact with dendritic spines of the biocytin-filled dendritic segments described above. We deter-

**Table 1. Quantitative analysis of CA1 pyramidal cell dendritic segments**

	Branch Order	Length, $\mu\text{m}$	Distance, $\mu\text{m}$ from cbl	Spine density, spines per $\mu\text{m}$	Filopodia density, filopodia per $\mu\text{m}$
OVX + O	2°	26.82	190	4.03	0.37
	3°	17.64	158	2.49	0.06
	3°	20.99	174	2.67	0.10
	3°	22.66	168	3.27	0.35
		$22.03 \pm 1.91$	$173 \pm 6.7$	$3.12 \pm 0.35$	$0.22 \pm 0.08$
OVX + E	2°	21.52	232	5.71	0.23
	3°	19.14	210	3.45	0.63
	3°	28.93	221	3.77	0.21
	3°	21.38	150	4.35	0.33
	3°	21.62	179	4.26	0.23
		$22.52 \pm 1.67$	$198 \pm 15.0$	$4.31 \pm 0.37$	$0.33 \pm 0.08$

Values represent data for individual dendritic segments. Treatment group averages  $\pm$  SEM are shown at the bottom of each column. The last OVX + O and OVX + E segments are shown in Fig. 3. cbl, cell body layer.

mined whether these boutons formed single or multiple synaptic contacts (i.e., were SSBs or MSBs) and which MSB contacts were same-cell or different-cell. Quantitative data for boutons in contact with each dendritic segment as well as treatment group averages are reported in Table 2.

Woolley *et al.* (5) proposed that estrogen-induced dendritic spines contact primarily preexisting boutons, transforming some previously SSBs into MSBs. Such a change would be predicted to increase numbers of MSB but not SSB contacts. Consistent with this prediction, we found that the linear density of SSB contacts was unchanged by estrogen treatment ( $t = -1.184$ ,  $P = 0.275$ ), whereas the linear density of MSB contacts was twice as high on OVX + E dendrites as on OVX + O dendrites (0.54 per  $\mu\text{m}$  in OVX + O vs. 1.10 per  $\mu\text{m}$  in OVX + E;  $t = -4.053$ ,  $P = 0.005$ ). Also consistent with Woolley *et al.* (5), the estrogen-induced increase in MSB density was paralleled by an increase in the relative proportion of MSBs to SSBs (18.2% in OVX + O vs. 28.2% in OVX + E;  $t = -3.26$ ,  $P = 0.014$ ).

Most MSBs reconstructed in the current analysis formed synapses with only two dendritic spines. Three-spine MSBs were slightly more frequent on OVX + E dendrites but were observed in both groups. Four-spine MSBs were observed only in contact with OVX + E dendrites. However, in contrast to the findings of Woolley *et al.* (5), there was no significant difference in the average number of synapses formed by MSBs in contact with OVX + O vs. OVX + E dendrites ( $t = 0.339$ ,  $P = 0.745$ ). The estrogen-induced difference in MSB density was accounted for largely by increased linear density of two-spine MSBs (0.461 per

$\mu\text{m}$  in OVX + O vs. 0.927 per  $\mu\text{m}$  in OVX + E;  $t = -3.671$ ,  $P = 0.008$ ). No significant differences were observed in the linear density of MSBs that formed more than two synapses ( $t = -1.1445$ ,  $P = 0.191$ ).

**Same-Cell vs. Different-Cell MSBs.** Analysis of same-cell vs. different-cell MSBs showed that the vast majority of MSBs in both treatment groups formed different-cell synaptic contacts. Among two-spine MSBs, very few formed both synapses with the filled cell, leading to a low linear density of same-cell two-spine MSBs, which was unchanged by estrogen treatment ( $t = -1.513$ ,  $P = 0.174$ ). In contrast, the linear density of two-spine MSBs that formed different-cell contacts was more than doubled by estrogen (0.42 per  $\mu\text{m}$  in OVX + O vs. 0.86 per  $\mu\text{m}$  in OVX + E;  $t = -3.847$ ,  $P = 0.006$ ).

The prevalence of different-cell contacts extended to MSBs that form more than two synapses. Of all of the possible synaptic contacts on three- and four-spine MSBs that could have been made with either the filled or an unfilled cell (i.e., excluding the one filled spine synapse necessary for inclusion), the majority in each group was made with an unfilled spine. Thus, considering all MSBs (two-, three-, and four-spine), the linear density of same-cell contacts was not affected by estrogen (0.09 per  $\mu\text{m}$  in OVX + O vs. 0.12 per  $\mu\text{m}$  in OVX + E;  $t = -0.686$ ,  $P = 0.514$ ), whereas the density of different-cell contacts made by synaptically connected MSBs was significantly greater on dendrites from estrogen-treated animals (0.52 per  $\mu\text{m}$  in OVX + O vs. 1.15 per  $\mu\text{m}$  in OVX + E;  $t = -3.674$ ,  $P = 0.008$ ). These contacts

**Table 2. Quantitative analysis of CA1 presynaptic boutons**

	SSB density, SSB per $\mu\text{m}$	MSB density, MSB per $\mu\text{m}$	Percentage of MSBs	Same-cell MSB contacts, MSB synapses per $\mu\text{m}$	Different-cell MSB contacts, MSB synapses per $\mu\text{m}$
OVX + O	2.98	0.71	19.2	0.22	0.60
	1.98	0.40	16.7	0.06	0.40
	2.10	0.43	17.0	0.00	0.52
	2.47	0.62	20.0	0.09	0.57
	$2.38 \pm 0.22$	$0.54 \pm 0.07$	$18.2 \pm 0.8$	$0.09 \pm 0.05$	$0.52 \pm 0.04$
OVX + E	4.23	1.30	23.5	0.19	1.30
	2.51	0.84	25.0	0.10	0.78
	2.56	0.90	26.0	0.10	0.86
	2.71	1.08	28.4	0.09	1.22
	2.45	1.39	38.3	0.14	1.57
	$2.89 \pm 0.34$	$1.10 \pm 0.11^{**}$	$28.2 \pm 2.6^{*}$	$0.12 \pm 0.02$	$1.15 \pm 0.15^{**}$

Values represent data for the same dendritic segments shown in Table 1, in the same order. Treatment group averages  $\pm$  SEM are shown at the bottom of each column. The last OVX + O and OVX + E segments are shown in Fig. 3. \*,  $P < 0.05$  from OVX + O; \*\*,  $P < 0.01$  from OVX + O.

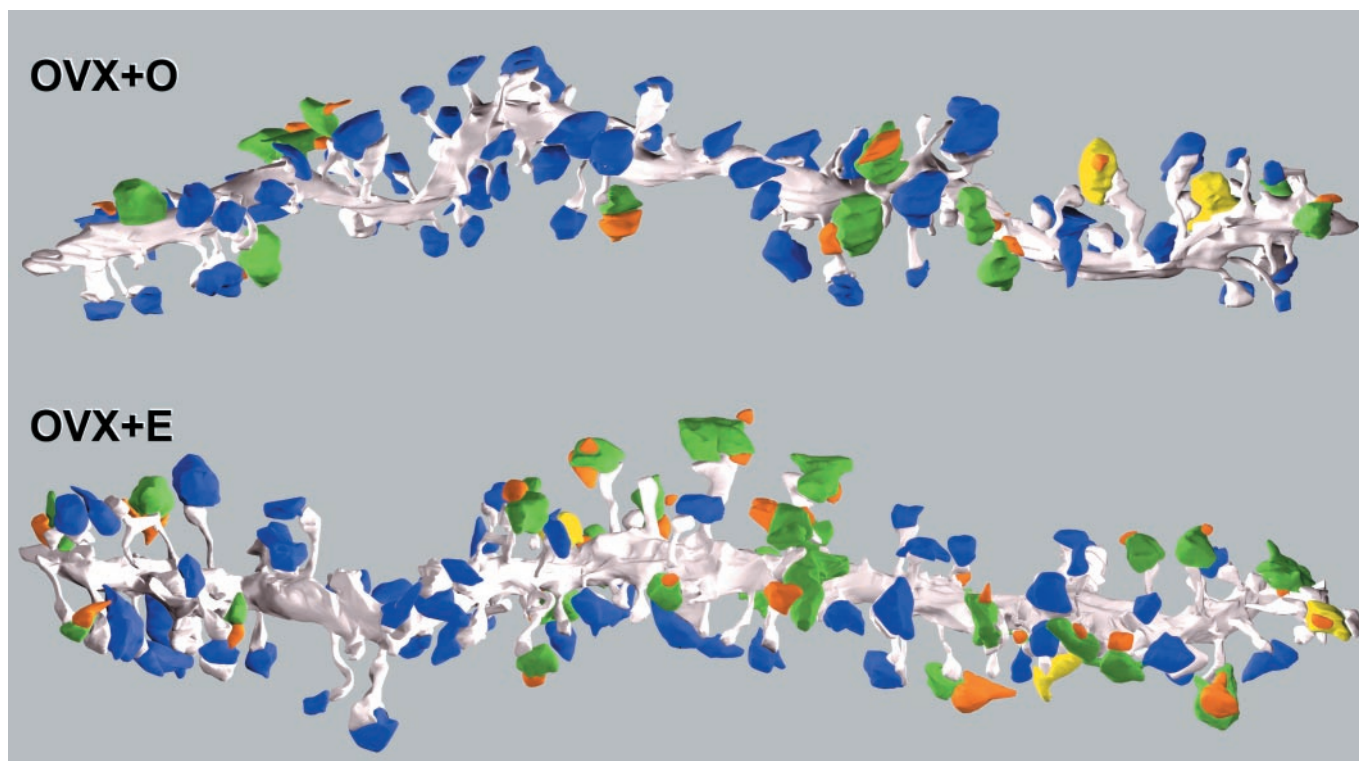


**Fig. 3.** Three-dimensional reconstructions of OVX + O and OVX + E dendritic segments. The dendrite is gray, SSBs are blue, different-cell MSBs are green, same-cell MSBs are yellow, and spines from other unfilled cells are orange. These are the last OVX + O and OVX + E dendrites in Tables 1 and 2. For the purpose of this figure, an MSB that made at least two synapses with the filled cell is shown as a same-cell MSB. Note the increase in dendritic spine and MSB density on the OVX + E dendrite, clustering of MSBs, and that the vast majority of MSBs are different-cell.

represent sites at which a postsynaptic cell shares the same presynaptic input with one or more other postsynaptic cells.

Fig. 3 shows examples of reconstructed dendritic segments including spines, presynaptic boutons, and unfilled spines synaptically connected to those presynaptic boutons from an OVX + O and an OVX + E animal.

**Linear Distribution of MSBs.** Serial reconstruction of individual dendrites and their presynaptic boutons also permitted analysis of the location of MSBs and SSBs along the length of dendritic segments. Interestingly, MSBs did not appear to be distributed randomly but occurred in clusters, particularly on dendrites from estrogen-treated animals (Figs. 3 and 4). Analysis of the order of

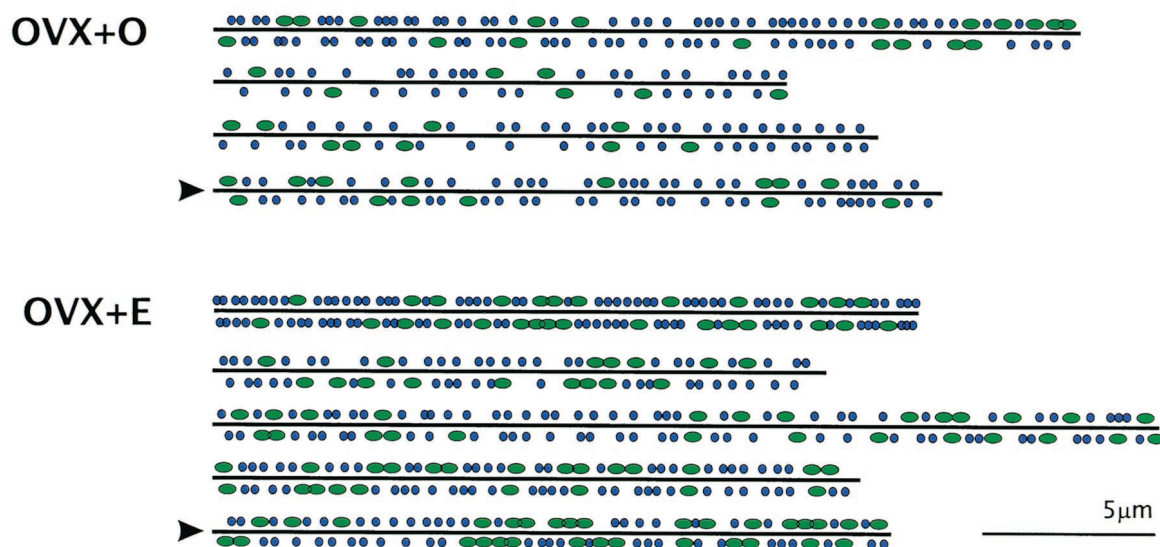


**Fig. 4.** Schematic diagrams showing the approximate location of SSBs (blue circles) and MSBs (green ovals) along the length of OVX + O and OVX + E dendritic segments. Boutons extending away from the viewer are included below the line; boutons extending toward the viewer are included above the line. The order of dendrites is the same as in Tables 1 and 2. Arrowheads mark the same dendrites shown in Fig. 3. Note the nonrandom sequence of MSBs.

occurrence of SSBs vs. MSBs along the length of each dendrite showed that in the majority of segments, MSB occurrence was significantly nonrandom ( $Z_U > 1.96$ ,  $P < 0.05$ ).

## Discussion

The principal finding of this study is that MSBs induced by estrogen reflect increased synaptic coupling of single presynaptic inputs to multiple postsynaptic CA1 pyramidal cells. In both estrogen-treated and control animals, a very high proportion of MSBs in synaptic contact with CA1 pyramidal cell dendritic spines form their additional synapses with different postsynaptic cells. The linear density of same-cell MSBs was quite low and not changed significantly by estrogen. In contrast, the linear density of different-cell MSBs was much greater, and different-cell MSB density was twice as high on dendrites from estrogen-treated animals as from controls. Thus, it appears that in addition to increasing the density of excitatory synaptic input to individual CA1 pyramidal cells (1–4), estrogen also increases the divergence of excitatory synaptic input from single presynaptic boutons to multiple postsynaptic cells.

That new dendritic spines seem to form synapses with boutons that are connected synaptically to different postsynaptic cells suggests that estrogen promotes the formation of new synaptic connections rather than the enhancement of existing connections. The possibility of new synaptic connections is exciting; however, an alternative that cannot be excluded at this point is that axons to which newly formed different-cell MSBs belong also form synapses elsewhere in the dendritic trees of postsynaptic cells that form new spine/MSB synapses and therefore are already synaptically connected to them.

In addition to greater understanding of same-cell vs. different-cell MSB relationships, we also observed a distinct spatial clustering of MSBs along the length of reconstructed dendritic segments. Indeed, we observed that the linear density of MSBs could vary widely within a dendritic segment. The nonrandom distribution of MSBs along CA1 dendrites may be significant for understanding estrogen-induced synapse formation. Currently it is unknown to what extent pre- vs. postsynaptic cells are responsible for initiating the formation of estrogen-induced synapses. Clustering of MSBs suggests spatial specificity of new synapses; new spine synapses may be formed in particular zones along the length of CA1 dendrites. If special properties of those zones can be identified, it will be a significant step toward understanding the mechanisms of spine/synapse formation in the adult brain.

The current study confirmed several previous observations of estrogen's effects on hippocampal synaptic connectivity. For example, even though only a small number of dendritic segments was analyzed here, the density of dendritic spines on the reconstructed dendrites from estrogen-treated animals was greater than on dendrites from control animals (1–4). Additionally, this study also replicated the estrogen-induced increase in

relative frequency of MSBs to SSBs (by 65% in this study vs. 60% in the ref. 5 study).

Although the results presented here are generally in agreement with previous studies, the overall frequency of MSBs and average number of synapses per MSB were lower in the current analysis than in ref. 5. Woolley *et al.* used these parameters to calculate a 25% increase in average synapses per bouton in estrogen-treated tissue. However, an analogous calculation based on data from the current study indicates a 10% increase. One possible explanation for a lower percentage difference in synapses per bouton is that some estrogen-induced synapses are formed with new SSBs, contrary to the suggestion of Woolley *et al.* (5). However, as discussed below, MSB clustering may lead to an inaccurate estimate of overall MSB frequency and synapse number when analyzing synapses formed along dendritic lengths.

The impact of MSB clustering on quantitative data from Woolley *et al.* (5) was likely to be minimal, because this study analyzed a large portion of all boutons within a particular volume of tissue. The current analysis reconstructed all boutons that were in synaptic contact with spines along a length of dendrite. This difference, coupled with a necessarily small number of reconstructed dendrites, makes it possible that the dendritic segments we reconstructed were not connected to a sufficiently representative distribution of MSB clusters to accurately quantify MSB frequency. Thus, many MSB clusters present in the volume of our series might not have been analyzed because none of their synapses were formed with the filled cell. Given the potential effects of MSB clustering on analysis of synapses along lengths of dendrite, data from Woolley *et al.* should be taken as the more accurate estimate of MSB frequency in the CA1 stratum radiatum. However, even though MSB clustering may have affected quantification of total numbers of MSBs in the current study, it is unlikely to have affected our conclusions regarding same-cell vs. different-cell MSBs, because same-cell MSBs were seen so rarely and generally were scattered within clusters of primarily different-cell MSBs.

The estrogen-induced increase in different-cell MSB contacts has important implications for hippocampal physiology, particularly if those MSBs reflect the establishment of new synaptic connections between previously unconnected cells. One of the most robust effects of estrogen on the hippocampus is a decrease in the threshold for seizure activity (e.g., refs. 9–11). The enhanced divergence of presynaptic input reported here is predicted to increase synchronization of synaptically driven activity in CA1. As such, these structural changes may contribute significantly to increasing susceptibility to synchronous discharge associated with seizures.

We thank Dr. Sandra Eyster for statistical advice and the Northwestern University Biological Sciences Electron Microscopy Facility. This work was supported by NS37324 (National Institute of Neurological Disorders and Stroke) and The Alfred P. Sloan Foundation.

1. Gould, E., Woolley, C. S., Frankfurt, M. & McEwen, B. S. (1990) *J. Neurosci.* **10**, 1286–1291.
2. Woolley, C. S. & McEwen, B. S. (1993) *J. Comp. Neurol.* **336**, 293–306.
3. Woolley, C. S. & McEwen, B. S. (1992) *J. Neurosci.* **12**, 2549–2554.
4. Woolley, C. S., Weiland, N. G., McEwen, B. S. & Schwartzkroin, P. A. (1997) *J. Neurosci.* **17**, 1848–1859.
5. Woolley, C. S., Wenzel, H. J. & Schwartzkroin, P. A. (1996) *J. Comp. Neurol.*

**373**, 108–117.

6. Sorra, K. E. & Harris, K. M. (1993) *J. Neurosci.* **13**, 3736–3748.
7. Schwartzkroin, P. A. (1975) *Brain Res.* **85**, 423–436.
8. Harris, K. M. & Stevens, J. K. (1989) *J. Neurosci.* **9**, 2982–2997.
9. Terasawa, E. & Timiras, P. S. (1968) *Endocrinology* **83**, 207–216.
10. Buterbaugh, G. G. & Hudson, G. M. (1991) *Exp. Neurol.* **111**, 55–64.
11. Woolley, C. S. (2000) *Epilepsia* **41**, 510–515.